

# High-performance and high-temperature continuous-wave-operation 1300 nm InGaAsN quantum well lasers by organometallic vapor phase epitaxy

Nelson Tansu<sup>a)</sup>

Center for Optical Technologies, Department of Electrical and Computer Engineering, Lehigh University, Sinclair Laboratory, 7 Asa Drive, Bethlehem, PA 18015 and Reed Center for Photonics, Department of Electrical Computer Engineering, University of Wisconsin-Madison, 1415 Engineering Drive, Madison, Wisconsin 53706-1691

Andrew Quandt, Manoj Kanskar, and William Mulhearn  
Alfalight, Inc., 1832 Wright Street, Madison, Wisconsin 53704

Luke J. Mawst

Reed Center for Photonics, Department of Electrical Computer Engineering, University of Wisconsin-Madison, 1415 Engineering Drive, Madison, Wisconsin 53706-1691

(Received 30 September 2002; accepted 12 May 2003)

Continuous-wave (cw) operation of organometallic vapor phase epitaxy-grown  $\text{In}_{0.4}\text{Ga}_{0.6}\text{As}_{0.995}\text{N}_{0.005}$  quantum well (QW) lasers has been realized, at a room-temperature near-threshold emission wavelength of  $1.295\ \mu\text{m}$ , with a threshold-current density of  $220\ \text{A}/\text{cm}^2$  for  $2000\ \mu\text{m}$  cavity-length ( $L_{\text{cav}}$ ) devices. A threshold current density of only  $615\ \text{A}/\text{cm}^2$  was achieved for cw operation at a temperature of  $100\ ^\circ\text{C}$ , with an emission wavelength of  $1.331\ \mu\text{m}$ . A maximum cw-output power of  $1.8\ \text{W}$  was obtained for InGaAsN QW lasers with cavity lengths of  $1000$  and  $2000\ \mu\text{m}$ , at a heat-sink temperature of  $20\ ^\circ\text{C}$ . © 2003 American Institute of Physics. [DOI: 10.1063/1.1591238]

The InGaAsN quantum well (QW) active region<sup>1–15</sup> on a GaAs substrate is a very promising alternative to the conventional InP-based technology<sup>16,17</sup> for realizing high-performance, high-temperature operation 1300 nm diode lasers. Conventional 1300 nm InGaAsP–InP lasers suffer from poor lasing performance at elevated temperature. This has been attributed to various mechanisms including Auger recombination, carrier leakage, intervalence-band absorption, and temperature-sensitive gain. Recently, organometallic vapor phase epitaxy (OMVPE) has been pursued extensively to achieve high performance InGaAsN QW lasers.<sup>3–7</sup> Only recently, OMVPE-grown InGaAsN QW lasers<sup>3–7</sup> operating at  $\lambda=1300\ \text{nm}$  have demonstrated performance comparable with the InGaAsN QW lasers grown with molecular beam epitaxy.<sup>8–12</sup>

We report the realization of very-low threshold-current density ( $J_{\text{th}}$ ) cw operation of strain-compensated OMVPE–InGaAsN QW lasers with a room-temperature ( $T=20\ ^\circ\text{C}$ ) near-threshold emission wavelength of  $1.295\ \mu\text{m}$ , up to operation temperatures of  $100\ ^\circ\text{C}$ . Threshold current density values, under cw operation and at an operation temperature of  $100\ ^\circ\text{C}$ , of only  $615\ \text{A}/\text{cm}^2$  were measured for InGaAsN QW lasers at a wavelength of  $1.331\ \mu\text{m}$ . A comparison of our OMVPE-grown InGaAsN QW lasers with existing published data from high performance 1300 nm QW lasers using conventional InP technology is also presented.

All the laser structures here were grown by low-pressure OMVPE. The group-V precursors are arsine ( $\text{AsH}_3$ ) and phosphine ( $\text{PH}_3$ ). The group-III precursors are the trimethyl

(TM–) sources of gallium (Ga), aluminum (Al), and indium (In). The N- precursor is commercial U-dimethylhydrazine (U–DMHy), and was used without any further treatment or purification process. The dopant sources are  $\text{SiH}_4$  and diethylzinc (DEZn) for the  $n$  and  $p$  dopants, respectively.

The laser structures studied here, as shown in Fig. 1, consist of a  $60\ \text{\AA}$  ( $\Delta a/a=2.7\%$ )  $\text{In}_{0.4}\text{Ga}_{0.6}\text{As}_{0.995}\text{N}_{0.005}$  single-QW active layer with GaAs layers bounding the QW. Partial strain compensation of the highly strained InGaAsN QW<sup>2,3,13,14</sup> is achieved by utilizing  $\text{GaAs}_{0.85}\text{P}_{0.15}$  tensile-strained layers offset from the QW,<sup>2</sup> and a tensile-strained buffer layer of  $\text{GaAs}_{0.67}\text{P}_{0.33}$ <sup>2,3</sup> as shown in Fig. 1. The benefit and purpose of the various strain compensating layers have been demonstrated and elaborated on in our earlier studies,<sup>2,3</sup> where we reported improved luminescence for the InGaAsN QW-active region employing the tensile-strained barriers and buffer layer. The lower- and top-cladding layers

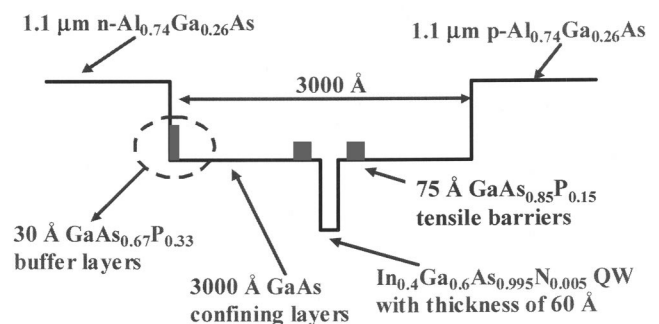


FIG. 1. Schematic energy band diagram for the  $\text{In}_{0.4}\text{Ga}_{0.6}\text{As}_{0.995}\text{N}_{0.005}$ – $\text{GaAs}_{0.85}\text{P}_{0.15}$  QW laser structure with a tensile-strained buffer layer consisting of  $30\ \text{\AA}$   $\text{GaAs}_{0.67}\text{P}_{0.33}$ .

<sup>a)</sup>Electronic mail: tansu@Lehigh.edu

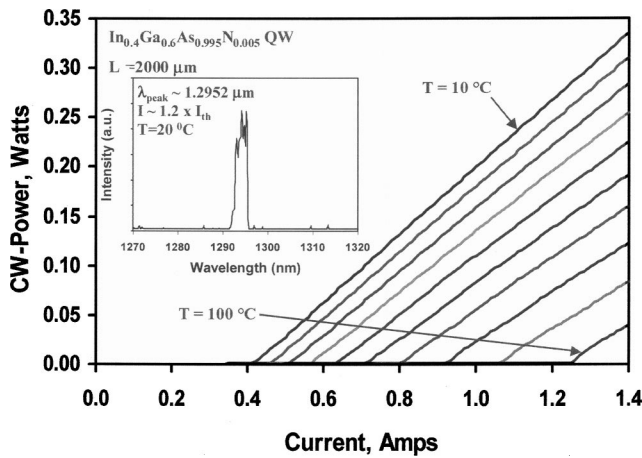


FIG. 2. The measured cw output power vs current-characteristics of the 1300 nm InGaAsN QW lasers with  $L_{cav}=2000 \mu\text{m}$ , as a function of temperature. The inset shows the near-threshold lasing spectrum at a heat-sink temperature of 20 °C.

of the lasers consist of  $\text{Al}_{0.74}\text{Ga}_{0.26}\text{As}$  layers with doping levels of  $1 \times 10^{18} \text{ cm}^{-3}$  for both the  $n$ - and  $p$ -cladding layers, respectively. The growth temperatures of the  $n$ - and  $p$ - $\text{Al}_{0.74}\text{Ga}_{0.26}\text{As}$  are 775 and 640 °C, respectively. The annealing of the InGaAsN QW is accomplished during the growth of the top cladding layer at a temperature of 640 °C, with duration of approximately 27 min. Because of the low incorporation efficiency of N into the InGaAsN QW, a very large [DMHy]/V ratio (as high as 0.961) is required to incorporate sufficient N into the QW to push the emission wavelength to 1300 nm, resulting in the requirement of a  $[\text{AsH}_3]/\text{III}$  ratio as low as 13–20.<sup>3</sup>

The 1300 nm InGaAsN QW lasers were characterized by measuring broad-area lasers with a stripe-width ( $w$ ) of 100  $\mu\text{m}$  and various cavity lengths ( $L_{cav}$ ). Under pulsed conditions (pulse width of 6  $\mu\text{s}$ , and 1% duty cycle) these devices demonstrate extremely low threshold-current density, with  $J_{th}$  as low as 211 and 453  $\text{A}/\text{cm}^2$  for cavity lengths of 2000 and 500  $\mu\text{m}$ , respectively. All of the pulsed characteristics of these lasers have been summarized in Table I of Ref. 3.

The cw operation characteristics of the InGaAsN QW lasers were measured from devices with facet coatings of high-reflective (HR) and antireflective (AR) layers. The HR layers consist of three pairs of  $\text{Al}_2\text{O}_3/\text{Si}$  with reflectivity in excess of 95%, and the AR layer was formed by a single layer of  $\text{Al}_2\text{O}_3$  with reflectivity estimated to be in the range of 7%–10%. Devices with cavity-lengths of 1000–2000  $\mu\text{m}$  were mounted junction down on copper heatsinks, and they were measured under cw operation at temperatures in the range of 10–100 °C.

The measured cw output-power ( $P_{out}$ ) characteristics, as a function of the injected-current ( $I$ ) and the heat-sink temperature ( $T$ ), are shown in Fig. 2. The cw characteristics of the InGaAsN-QW lasers are measured up to a temperature of 100 °C, limited by our equipment. The near-threshold ( $I \sim 1.1$ – $1.2 I_{th}$ ) emission wavelengths of the lasers with a cavity length of 2000  $\mu\text{m}$  are measured as 1295.2 and 1331 nm, at temperatures of 20 and 100 °C, respectively.

The measured threshold current density of the HR/AR-coated InGaAsN-QW lasers under cw operation is very comparable with that of the as-cleaved lasers, as shown in

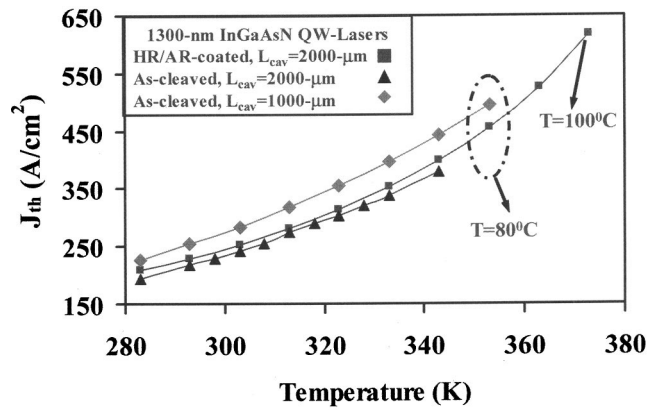


FIG. 3. The measured threshold-current densities of the InGaAsN QW lasers as a function of temperature, for as-cleaved and HR/AR-coated devices with  $L_{cav}=1000$ – $2000 \mu\text{m}$ .

Fig. 3. These similarities in the threshold characteristics of the HR/AR-coated devices and the as-cleaved devices are attributed to the fact that the dominant loss in our lasers is the large internal loss (approximately  $13 \text{ cm}^{-1}$ ). The total mirror loss [ $\alpha_m = (1/2L)\ln(1/\{R_1R_2\})$ ] of the HR/AR coated devices ( $\alpha_m \sim 6.0$ – $6.8 \text{ cm}^{-1}$ ,  $L_{cav}=2000 \mu\text{m}$ ) is comparable with that of the as-cleaved devices ( $\alpha_m = 6.2 \text{ cm}^{-1}$ ,  $L_{cav}=2000 \mu\text{m}$ ). Despite the large internal loss, the threshold-current density of the lasers with a cavity length of 2000  $\mu\text{m}$  is measured as 210–220  $\text{A}/\text{cm}^2$ , at a temperature of 20 °C under cw operation. At elevated temperatures of 80 and 100 °C, the threshold current densities of the HR/AR-coated ( $L_{cav}=2000 \mu\text{m}$ ) lasers are measured as only 455 and 615  $\text{A}/\text{cm}^2$ , respectively, under cw operation.

To compare the lasing performance of the 1300 nm InGaAsN QW lasers with those of the conventional InP technology, we show the published results that represent some of the best-performing 1300 nm diode lasers based on InGaAsP-QWs<sup>16</sup> and InGaAlAs-QWs<sup>17</sup> in Fig. 4. Due to the low material gain parameter, carrier leakage, and Auger recombination, typical 1300 nm InGaAsP-InP QW lasers require 9–14 QWs.<sup>16</sup> The 1300 nm InGaAlAs QW lasers require approximately 4–6 QWs for optimized structures.<sup>17</sup>

For optimized 1300 nm InGaAsP-QW structures,<sup>16</sup> threshold current densities of approximately 1650–1700

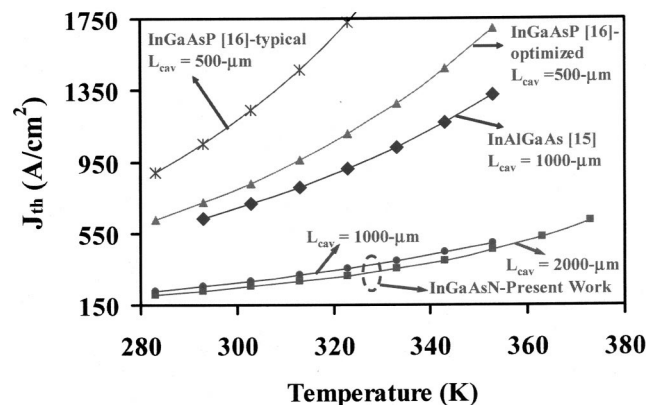


FIG. 4. The measured threshold-current densities of the as-cleaved diode lasers for the 1300 nm InGaAsN QW lasers ( $L_{cav}=1000$ – $2000 \mu\text{m}$ ) and the best-reported 1300 nm InGaAsP-QW ( $L_{cav}=500 \mu\text{m}$ ) and InGaAlAs-QW ( $L_{cav}=1000 \mu\text{m}$ ) lasers as a function of temperature.

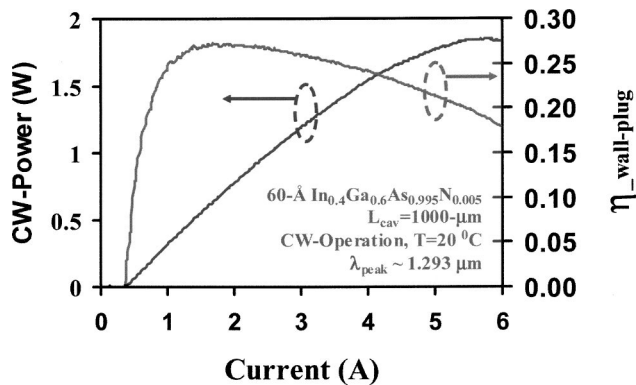


FIG. 5. The measured cw power vs current characteristic and total power conversion efficiency (wall-plug efficiency) of an  $\text{In}_{0.4}\text{Ga}_{0.6}\text{As}_{0.995}\text{N}_{0.005}\text{-GaAs}_{0.85}\text{P}_{0.15}$  QW laser with  $L_{\text{cav}}=1000 \mu\text{m}$ , at a heat-sink temperature of  $20^\circ\text{C}$ .

$\text{A}/\text{cm}^2$  were achieved for devices with a cavity length of  $500 \mu\text{m}$  at an operation temperature of  $80^\circ\text{C}$ , as reported by Belenky *et al.*<sup>16</sup> The threshold current density of the  $1300 \text{ nm}$  diode lasers based on the InGaAlAs QW on InP, with a cavity length of  $1000 \mu\text{m}$ , has been reported as approximately  $1350 \text{ A}/\text{cm}^2$  at a temperature of  $80^\circ\text{C}$ .<sup>17</sup> The InGaAsN QW lasers require only a single QW active region for high temperature operation, owing to the larger material gain parameter and better electron confinement in the QW. Our  $1300 \text{ nm}$  InGaAsN single-QW as-cleaved diode lasers, with cavity lengths of  $500$  and  $1000 \mu\text{m}$ , have threshold current densities of only  $940$  and  $490 \text{ A}/\text{cm}^2$ , respectively, at a heat-sink temperature of  $80^\circ\text{C}$ .

The maximum cw output powers achievable from the  $1300 \text{ nm}$  InGaAsN-QW lasers are approximately  $1.8 \text{ W}$  for devices with cavity lengths of both  $1000$  and  $2000 \mu\text{m}$ , at heat-sink temperatures of  $20^\circ\text{C}$ . Figure 5 shows the measured output power versus current characteristic for devices with  $L_{\text{cav}}=1000 \mu\text{m}$ . This result represents the highest cw-output power reported for  $1300 \text{ nm}$  InGaAsN QW lasers grown by OMVPE at a heat-sink temperature of  $20^\circ\text{C}$ . The maximum total power conversion efficiency for devices with a cavity length of  $1000 \mu\text{m}$  is approximately  $28\%$ , and is limited by the large internal loss ( $\alpha_i=13 \text{ cm}^{-1}$ ) resulting from the narrow SCH region and relatively high doping level ( $1\text{-}2 \times 10^{18} \text{ cm}^{-3}$ ) of the  $p$  cladding of the laser. Further improvement by utilizing a broad-waveguide design should allow the realization of higher output power InGaAsN-QW lasers.

In summary, high-performance continuous-wave opera-

tion strain-compensated  $\text{In}_{0.4}\text{Ga}_{0.6}\text{As}_{0.995}\text{N}_{0.005}$  QW lasers, with room-temperature near-threshold lasing emission wavelength of  $1.295 \mu\text{m}$ , have been achieved by OMVPE utilizing  $\text{AsH}_3$  as the As precursor. The cw lasing threshold current densities of these devices ( $L_{\text{cav}}=2000 \mu\text{m}$ , with HR/AR coating) are  $200$  and  $615 \text{ A}/\text{cm}^2$ , at temperatures of  $20$  and  $100^\circ\text{C}$ , respectively. This result represents the lowest threshold current density for  $1300 \text{ nm}$  QW lasers under cw operation at temperatures up to  $100^\circ\text{C}$ , by comparison with reported results of the conventional InGaAsP and InAlGaAs  $1300 \text{ nm}$  QW lasers. Maximum cw output powers of  $1.8 \text{ W}$  were achieved for both  $1000$  and  $2000 \mu\text{m}$  cavity length devices at a heat-sink temperature of  $20^\circ\text{C}$ , which represents the highest cw output powers for  $1300 \text{ nm}$  OMVPE-grown InGaAsN QW lasers.

The authors would like to acknowledge helpful technical assistance from John Ochsner, and Edward Boyer, of Al-falight, Inc., Madison, WI.

- <sup>1</sup>M. Kondow, T. Kitatani, S. Nakatsuka, M. C. Larson, K. Nakahara, Y. Yazawa, M. Okai, and K. Uomi, *IEEE J. Sel. Top. Quantum Electron.* **3**, 719 (1997).
- <sup>2</sup>N. Tansu and L. J. Mawst, *IEEE Photonics Technol. Lett.* **14**, 444 (2002).
- <sup>3</sup>N. Tansu, N. J. Kirsch, and L. J. Mawst, *Appl. Phys. Lett.* **81**, 2523 (2002).
- <sup>4</sup>T. Takeuchi, Y.-L. Chang, M. Leary, A. Tandon, H.-C. Luan, D. P. Bour, S. W. Corzine, R. Twist, and M. R. Tan, *IEEE LEOS 2001 Post-Deadline Session*, 2001.
- <sup>5</sup>S. Sato, *Jpn. J. Appl. Phys., Part 1* **39**, 3403 (2000).
- <sup>6</sup>M. Kawaguchi, T. Miyamoto, E. Gouardes, D. Schlenker, T. Kondo, F. Koyama, and K. Iga, *Jpn. J. Appl. Phys., Part 2* **40**, L744 (2001).
- <sup>7</sup>F. Hohnsdorf, J. Koch, S. Leu, W. Stolz, B. Borchert, and M. Druminski, *Electron. Lett.* **35**, 571 (1999).
- <sup>8</sup>D. A. Livshits, A. Yu. Egorov, and H. Riechert, *Electron. Lett.* **36**, 1381 (2000).
- <sup>9</sup>J. Wei, F. Xia, C. Li, and S. R. Forrest, *IEEE Photonics Technol. Lett.* **14**, 597 (2002).
- <sup>10</sup>K. D. Choquette, J. F. Klem, A. J. Fischer, O. Blum, A. A. Allerman, I. J. Fritz, S. R. Kurtz, W. G. Breiland, R. Sieg, K. M. Geib, J. W. Scott, and R. L. Naone, *Electron. Lett.* **36**, 1388 (2000).
- <sup>11</sup>W. Ha, V. Gambin, M. Wistey, S. Bank, S. Kim, and J. S. Harris, Jr., *IEEE Photonics Technol. Lett.* **14**, 591 (2002).
- <sup>12</sup>C. S. Peng, T. Jouhti, P. Laukkanen, E.-M. Pavelescu, J. Konttinen, W. Li, and M. Pessa, *IEEE Photonics Technol. Lett.* **14**, 275 (2002).
- <sup>13</sup>N. Tansu and L. J. Mawst, *IEEE Photonics Technol. Lett.* **13**, 179 (2001).
- <sup>14</sup>N. Tansu, Y. L. Chang, T. Takeuchi, D. P. Bour, S. W. Corzine, M. R. T. Tan, and L. J. Mawst, *IEEE J. Quantum Electron.* **38**, 640 (2002).
- <sup>15</sup>N. Tansu and L. J. Mawst, *IEEE Photonics Technol. Lett.* **14**, 1052 (2002).
- <sup>16</sup>G. L. Belenky, C. L. Reynolds, Jr., D. V. Donetsky, G. E. Shtengel, M. S. Hybertsen, M. A. Alam, G. A. Baraff, R. K. Smith, R. F. Kazarinov, J. Winn, and L. E. Smith, *IEEE J. Quantum Electron.* **35**, 1515 (1999).
- <sup>17</sup>P. Savolainen, M. Toivonen, P. Melanen, V. Vilokinen, M. Saarinen, S. Orsila, T. Kuuslahti, A. Salokatve, H. Asonen, T. Panarello, R. Murison, and M. Pessa, in *Proc. 11th IPRM 1999*, 1999, paper MoP09.